JSR JOURNAL OF
SYNCHROTRON
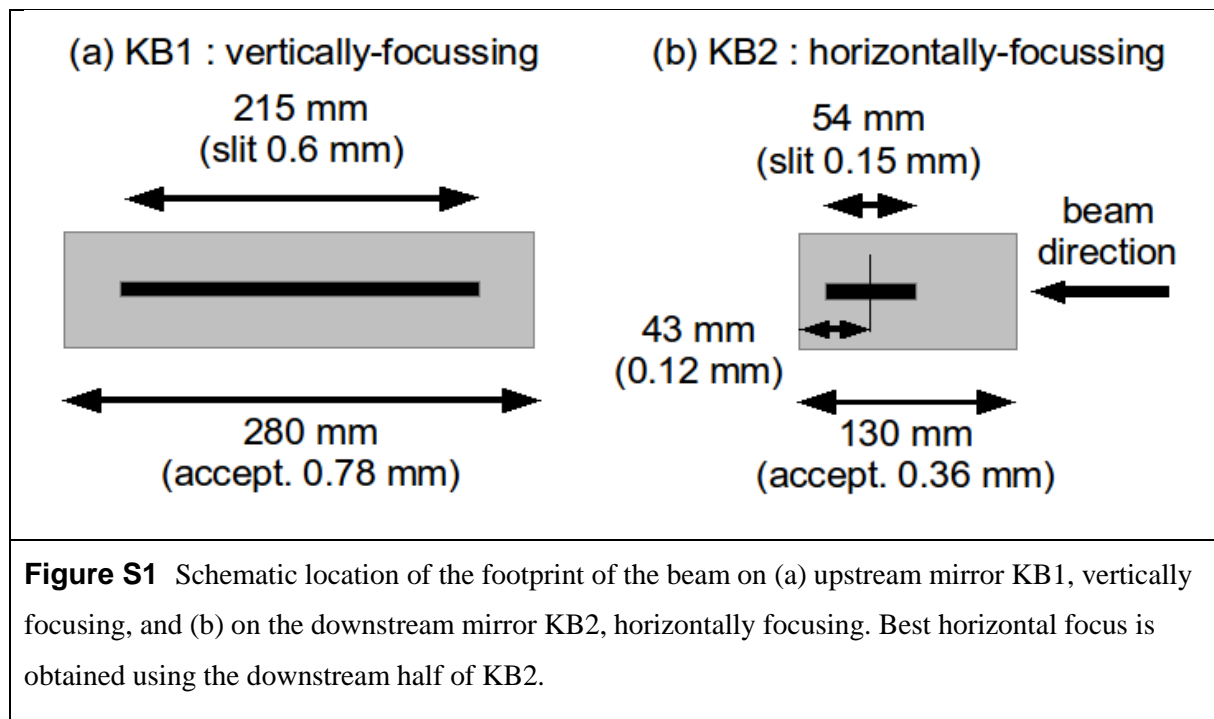RADIATION

Volume 23 (2016)

Supporting information for article:

KB-scanning of X-ray beam for Laue microdiffraction on accelero-phobic samples: application to *in situ* mechanically loaded nanowires

C. Leclere, T. W. Cornelius, Z. Ren, O. Robach, J.-S. Micha, A. Davydok, O. Ulrich, G. Richter and O. Thomas
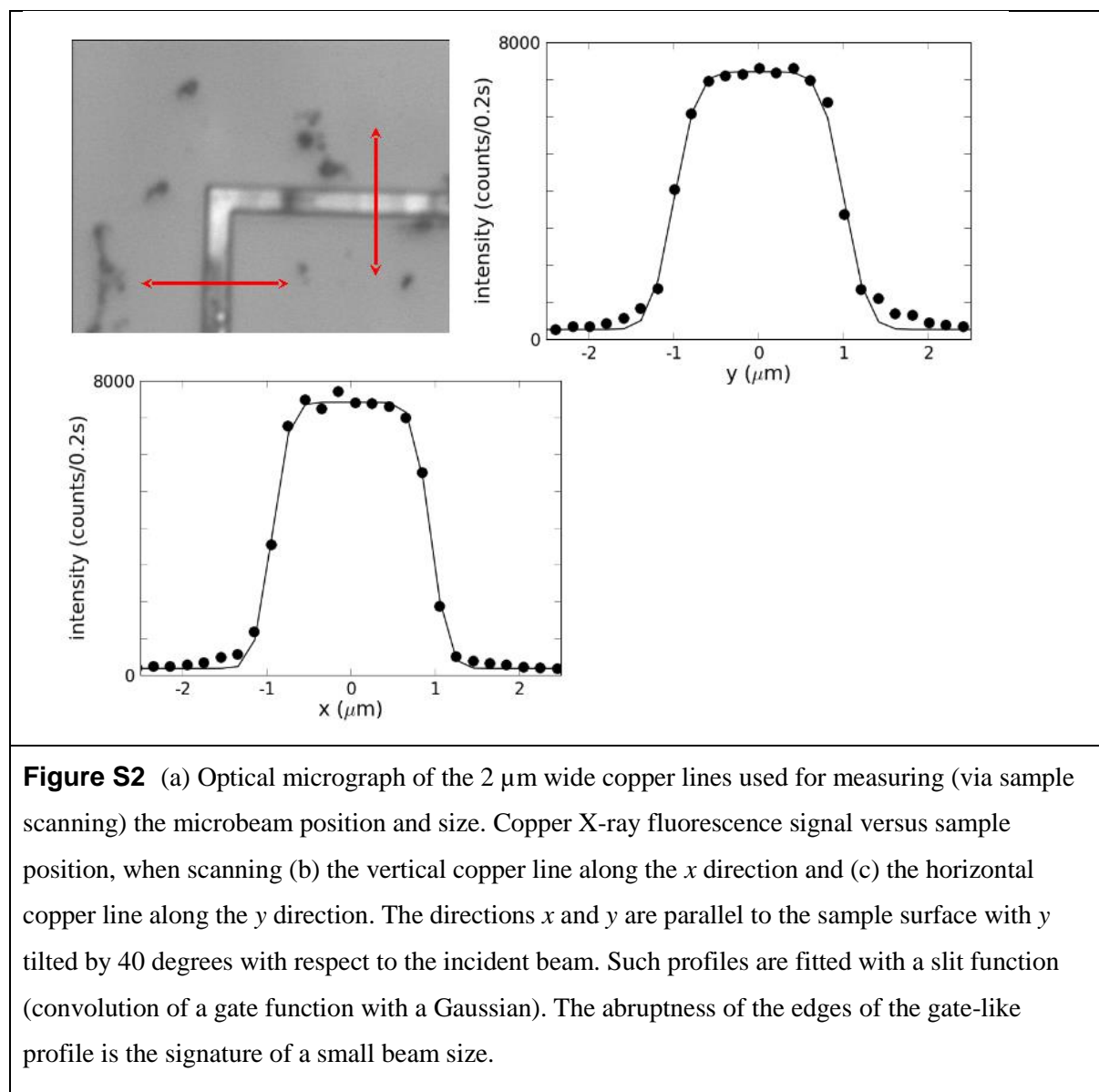
S1. Beam footprint on KB mirrors

Figures S1a and b show the footprint of the beam on the surface of the two mirrors in the "best focus" configuration.

Figure S1 Schematic location of the footprint of the beam on (a) upstream mirror KB1, vertically focusing, and (b) on the downstream mirror KB2, horizontally focusing. Best horizontal focus is obtained using the downstream half of KB2.

S2. Calibration of pseudo-motors for scanning of KB mirrors

For each of the KB scanning approaches, the beam-scanning pseudo-motor had to be calibrated, by measuring the displacement of the X-ray beam on the sample surface as a function of the displacement of the hexapods carrying the KB mirrors. For vertical (horizontal) beam displacements, a horizontal (vertical) copper line was scanned along y (x). An optical micrograph of the copper lines and typical linear scans across such lines are presented in figure S2.
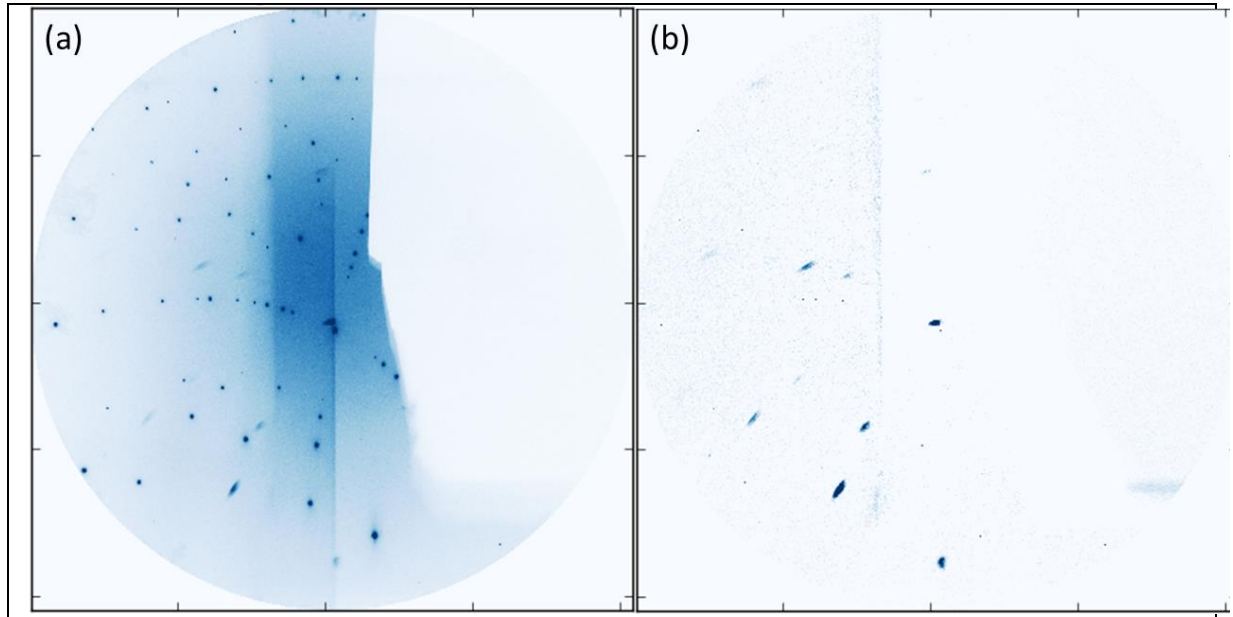

Figure S2 (a) Optical micrograph of the 2 µm wide copper lines used for measuring (via sample scanning) the microbeam position and size. Copper X-ray fluorescence signal versus sample position, when scanning (b) the vertical copper line along the x direction and (c) the horizontal copper line along the y direction. The directions x and y are parallel to the sample surface with y tilted by 40 degrees with respect to the incident beam. Such profiles are fitted with a slit function (convolution of a gate function with a Gaussian). The abruptness of the edges of the gate-like profile is the signature of a small beam size.

S3. Laue diffraction pattern

Figure S3 (a) Typical Laue microdiffraction pattern taken with the X-ray microbeam at the center of the most deformed Au nanowire. Two patterns are visible, the intense pattern of the Si substrate with about 80 spots and the weaker Au nanowire pattern with about 20 spots. (b) The same diffraction pattern after subtracting the Si peaks.

S4. Profile of a bent beam for different boundary conditions

In 1959, Landau *et al.* calculated the equilibrium equation for a bent beam, where each element along the beam is described by the following equation:

$$\frac{d\vec{M}}{dl} = \vec{F} \times \vec{t}$$

Here, $\vec{F}$ is the applied force, $\vec{M}$ is the momentum of internal stresses on the cross-section, $\vec{t}$ is the unit vector along the direction of the element, and l is the length of the element along the beam.

For small deflections, i.e. deflections smaller than the half-width of the beam, this equation can be simplified to the Euler-Bernoulli equation:

$$EI\frac{d^4w}{dx^4} = q \tag{S.1}$$

where w is the deflection of the beam, x is the position along the beam, E is the Young's modulus of the material, I is the second moment of inertia, and q is the force per unit length.
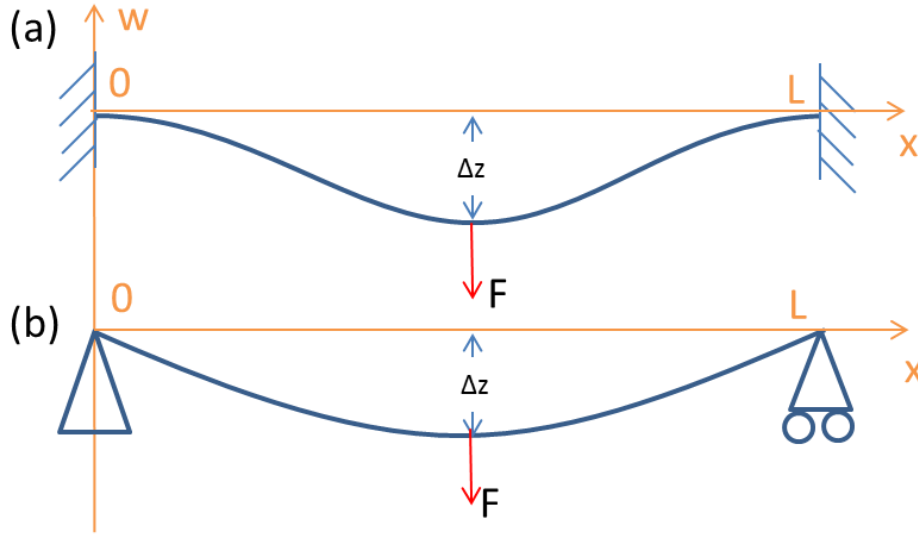
Figure S4 Schematic of the three point bending test on (a) a doubly-clamped and (b) a simply supported beam.

For different boundary conditions, this equation can be analytically solved generating the deformation profile of the beam $w(x)$. The three point bending test performed in our experiment (as illustrated in Fig. S4) can be described with a point load applied in the center of the beam ($q= -F\delta(x-L/2)$). Here, two kinds of boundary conditions are discussed: (i) doubly-clamped and (ii) simply supported boundary conditions. While in the first case both ends of the beam are fixed, the beam can freely tilt and slide along the support in the second case. The analytical solution of equation (S1) for the doubly-clamped beam is

$$
\begin{cases}
w = -\dfrac{Fx^2(3L - 4x)}{48EI} & for\ 0 \leq x \leq L/2 \\[2mm]
w = -\dfrac{F(L - x)^2(4x - L)}{48EI} & for\ L/2 \leq x \leq L
\end{cases}
$$

While the solution for the simply supported boundary condition ($d^2w/dx^2=0$, $d^3w/dx^3=0$) is

$$
\begin{cases}
w = -\dfrac{Fx(3L^2 - 4x^2)}{48EI} & for\ 0 \leq x \leq L/2 \\[2mm]
w = -\dfrac{F(L - x)(3L^2 - 4(L - x)^2)}{48EI} & for\ L/2 \leq x \leq L
\end{cases}
$$

The deformation profile for the Au nanowire under study with a width of 300 nm, a thickness of 100 nm, a length L of 8 μm, Young's modulus E of 79 GPa, and the applied force F of 50 nN is presented in Fig. S5(a) and (b) considering a doubly-clamed and a simply supported beam, respectively. By

calculating the first derivative of the deflection along the beam, the bending angle θ is deduced as shown in the Fig. S5 (c) and (d).
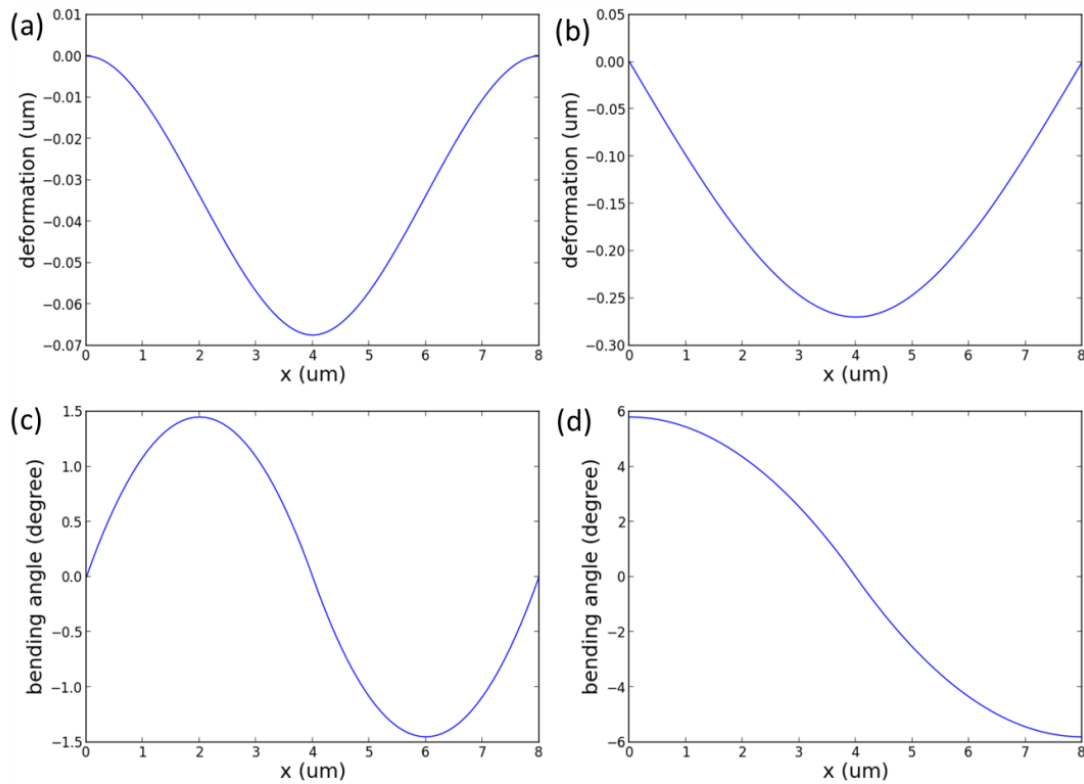

Figure S5 Deformation along a three-point bent beam for (a) doubly-clamped and (b) simply supported boundary conditions. Bending angle along the same beam (c) with clamped boundary conditions and (d) with simply supported boundary conditions.

For the same applied force, the simply supported beam exhibits a larger deflection than a doubly-clamped beam. In addition, simply supported boundary conditions result in maximal bending angles at the positions near the support, whereas the bending angle for doubly-clamped beams shows a sinusoidal behavior with maxima at half-distance between the loading point and the two supports. In the work presented in this article the bending angle exhibits a profile similar to the case of a doubly-clamped beam indicating that the nanowire is thoroughly fixed at the Si supports.